



# FRACTURE MECHANICS OF COMPOSITES WITH RESIDUAL STRESSES, IMPERFECT INTERFACES, AND TRACTION-LOADED CRACKS

John A. Nairn

Material Science and Engineering, University of Utah, Salt Lake City, Utah 84112, USA  
(e-mail: John.Nairn@m.cc.utah.edu)

(Submitted 31 October 2000)

## Abstract

By partitioning the total stresses in a damaged composite into either mechanical and residual stresses or into initial and perturbation stresses, it was possible to derive two exact results for the energy release rate due to crack growth. These general results automatically include the effects of residual stresses, traction-loaded cracks, and imperfect interfaces. These effects are normally not needed in fracture mechanics of homogeneous materials, but they are commonly needed for fracture mechanics of composites. The general results were used to consider mode I fracture in composites, fracture and thermal cracking for two-phase, isotropic composites, and interfacial fracture in the microbond and single-fiber, pull out tests. The analysis of interfacial fracture illustrates the importance of including friction effects in the energy release rate and not as part of the toughness of the composite. Many composite damage modes consist of a series of events instead of stable crack propagation. A new analysis method called finite fracture mechanics is proposed that predicts that the next event occurs when the total energy released by that event exceeds some critical value or toughness for that type of event. A finite fracture mechanics model for microcracking that can correlate the results from many laminates is described.

## 1 INTRODUCTION

A complete damage analysis of a composite material can be divided into two fields which are referred to here as *Damage Mechanics* and *Fracture Mechanics*. Damage mechanics refers to the problem of analyzing a composite with a fixed amount of damage and calculating the effective thermomechanical properties in the presence of that damage. Effective properties are often denoted with an asterisk as in  $S^*$ ,  $C^*$ , or  $\alpha^*$  for effective compliance, stiffness, and thermal expansion tensors, respectively. Fracture mechanics refers to the problem of considering a composite with a certain amount of damage and predicting the conditions for which the amount of damage will increase. Fracture mechanics typically involves calculating the energy release rate,  $G$ , for damage growth and then predicting that damage will grow when  $G$  exceeds the critical energy release rate,  $G_c$ , or toughness of the material. A complete damage analysis normally involves using both damage mechanics and fracture mechanics methods. First damage mechanics is used to calculate effective properties for a certain amount of damage. Second, the energy release rate is calculated; this step can often be done in terms of effective properties but typically requires derivatives of those properties with respect to damage area  $A$  (e.g.,  $dS^*/dA$ ,  $dC^*/dA$ , and  $d\alpha^*/dA$ ). Third, once energy release rate is known, fracture mechanics is used to predict the development of new damage. This last step leads to a new amount of damage and the entire process can begin again at step one with a damage mechanics analysis of the new damage state. The cyclic process and the relation between damage mechanics and fracture mechanics are illustrated in Fig. 1.

This paper focuses on the fracture mechanics part of a complete damage analysis and specifically focuses on calculation of the energy release rate for damage propagation. The required energy release rate can be

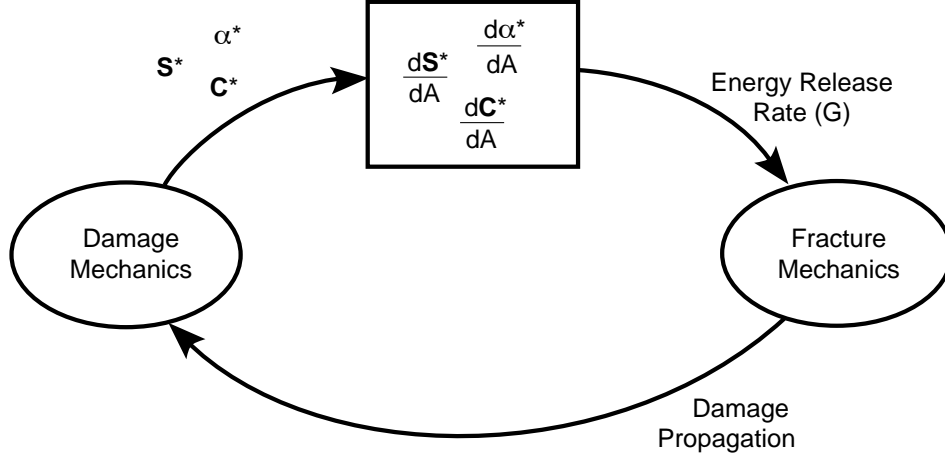


**Fig. 1.** A complete damage analysis of a composite material requires a coupling of damage mechanics and fracture mechanics. Damage mechanics is used to predict the effect of damage on effective properties. Fracture mechanics can use those effective properties to calculate energy release rate and therefore to predict propagation of damage.

calculated from a global energy balance using

$$G = -\frac{d\Pi}{dA} = \frac{d(W - U)}{dA} \quad (1)$$

where  $\Pi$  is thermoelastic potential energy,  $W$  is external work,  $U$  is thermoelastic internal energy, and  $dA$  is an increment in total crack area.<sup>1</sup> For uniaxial loading, many fracture mechanics books derive a result for  $G$  in terms of the effective compliance,  $C^*$ , or effective modulus,  $E^*$ , in the loading direction of<sup>1</sup>

$$G = \frac{P^2}{2} \frac{dC^*}{dA} \quad \text{or} \quad G = \frac{\sigma^2 V}{2} \frac{d(1/E^*)}{dA} \quad (2)$$

where  $P$  and  $\sigma$  are applied load and stress and  $V$  is specimen volume. For multi-axial loading, these uniaxial results can easily be generalized to

$$G = \frac{V}{2} \boldsymbol{\sigma} \cdot \frac{d\mathbf{S}^*}{dA} \boldsymbol{\sigma} \quad (3)$$

where  $\boldsymbol{\sigma}$  is the externally applied stress tensor and  $\mathbf{S}^*$  is the effective compliance tensor. Unfortunately, these basic results are almost never correct for analysis of composite fracture. A closer inspection reveals that they are *special-case* results that apply only for specimens with no residual stresses, for traction-free crack surfaces, and for composite materials with perfect interfaces. In contrast, due to a mismatch in thermal expansion coefficients between phases, composite materials inevitably develop residual stresses as they cool from processing temperatures to room temperature.<sup>2</sup> It is common for cracks in composites to be diverted along certain structural features in such a way that the crack surfaces may retain traction (*e.g.*, frictional contact between two fracture surfaces). Finally, composites always have interfaces between their phases. Some of those interfaces may be imperfect<sup>3</sup> or there may be *interphase* effects; both of these phenomena can influence the energy release rate.

The general problem of calculating energy release rate for composite fracture that includes effects of residual stresses, imperfect interfaces, and traction-loaded cracks has recently been considered in Ref. 4. The general approach is to partition total stresses into mechanical stresses ( $\boldsymbol{\sigma}^m$  with associated mechanical displacements  $\vec{u}^m$  and tractions  $\vec{T}^m$ ) and residual stresses ( $\boldsymbol{\sigma}^r$  with associated displacements  $\vec{u}^r$  and tractions  $\vec{T}^r$ ). By substituting the partitioned stresses into eqn (1) followed by several uses of virtual work and divergence theorems (details in Ref. 4), it is possible to derive the a general energy release rate result of

$$G = G_{mech} + \frac{VT}{2} \left( 2 \frac{d\langle \boldsymbol{\sigma}^m \cdot \boldsymbol{\alpha} \rangle}{dA} + \frac{d\langle \boldsymbol{\sigma}^r \cdot \boldsymbol{\alpha} \rangle}{dA} \right) + \frac{d}{dA} \left( \int_{S_c} \vec{T}^r \cdot \vec{u}^m dS + \frac{1}{2} \int_{S_c} \vec{T}^r \cdot \vec{u}^r dS \right) \quad (4)$$

where  $G_{mech}$  is the mechanical energy release rate or the energy release rate when  $T = 0$ :

$$G_{mech} = \frac{d}{dA} \left( \frac{1}{2} \int_{S_T} \vec{T}^0 \cdot \vec{u}^m dS - \frac{1}{2} \int_{S_u} \vec{T}^m \cdot \vec{u}^0 dS + \frac{1}{2} \int_{S_c} \vec{T}^m \cdot \vec{u}^m dS \right) \quad (5)$$

and angle brackets indicates a averaged a quantity over the total volume,  $V$ , of the specimen:

$$\langle f(x, y, z) \rangle = \frac{1}{V} \int_V f(x, y, z) dV \quad (6)$$

Here  $T = T_s - T_0$  is the difference between the specimen temperature and the stress-free temperature,  $\vec{T}^0$  are tractions applied over the boundary surface area  $S_T$ ,  $\vec{u}^0$  are the fixed displacements imposed on the boundary surface area  $S_u$ , and  $S_c$  includes all crack and interfacial surfaces. Equation (4) is exact for composite fracture. The first term ( $G_{mech}$ ) is the traditional energy release rate that considers only mechanical stresses. The second term accounts for residual stresses.<sup>5</sup> The subsequent terms, which are integrals over  $S_c$ , account for traction-loaded cracks and imperfect interfaces.

Instead of partitioning into mechanical and residual stresses, sometimes it is more useful to partition total stresses into initial stress,  $\sigma^0$ , and perturbation stresses,  $\sigma^p$ . In this partitioning,  $\sigma^0$  are the stresses in a composite, which may include some initial state of damage, and  $\sigma^p$  are the *change* in those stresses caused by the propagation of damage. By substituting initial and perturbation stresses into eqn (1) and making use of virtual work and divergence theorems (details in Ref. 4), it is possible to derive a second energy release rate theorem:

$$G = \frac{d}{dA} \left( \int_{S_c} \vec{T}^p \cdot \vec{u}^0 dS + \frac{1}{2} \int_V \sigma^p \mathbf{S} \sigma^p dV \right) \quad (7)$$

where  $\vec{T}^p$  and  $\vec{u}^0$  are the tractions associated with the perturbation stresses and the displacements associated with the initial stresses on the crack and interface surfaces, respectively.

This paper considers application of the mechanical and residual stress partitioning for analysis of crack growth in composites and analysis of interfacial fracture. The partitioning into initial and perturbation stresses is used to develop a new fracture mechanics method, called finite fracture mechanics, that is a potential tool for predicting fracture events in composites.

## 2 RESULTS AND EXAMPLES

### 2.1 Mode I Fracture

Some powerful simplifications are possible when the crack growth in a composite proceeds by pure mode I fracture (or similarly, but less commonly, by pure mode II or III fracture). In Ref. 4, it was argued that during mode I crack growth, the energy release rate must scale with mode I stress intensity factor squared,  $K_I^2$ . Furthermore, for linear elastic materials in which all applied tractions and displacements are scaled by a factor  $P$  and the temperature difference  $T$  is scaled by a factor  $T^*$ ,  $K_I$  must scale by a linear combination of  $P$  and  $T^*$ , which leads to

$$G_I \propto K_I^2 = (c_1 P + c_2 T^*)^2 \quad (8)$$

Comparing eqn (8) to eqn (4) similarly scaled by  $P$  and  $T^*$ , we can prove that

$$\frac{\frac{VT}{2} \frac{d \langle \sigma^m \cdot \alpha \rangle}{dA} + \frac{1}{2} \frac{d}{dA} \int_{S_c} \vec{T}^r \cdot \vec{u}^m dS}{G_{mech}} = \frac{\frac{VT}{2} \frac{d \langle \sigma^r \cdot \alpha \rangle}{dA} + \frac{1}{2} \frac{d}{dA} \int_{S_c} \vec{T}^r \cdot \vec{u}^r dS}{\frac{VT}{2} \frac{d \langle \sigma^m \cdot \alpha \rangle}{dA} + \frac{1}{2} \frac{d}{dA} \int_{S_c} \vec{T}^r \cdot \vec{u}^m dS} \quad (9)$$

Substitution into eqn (4) gives the pure mode I energy release rate of:<sup>4</sup>

$$\frac{G_I}{G_{mech}} = \left( 1 + \frac{\frac{VT}{2} \frac{d \langle \sigma^m \cdot \alpha \rangle}{dA} + \frac{1}{2} \frac{d}{dA} \int_{S_c} \vec{T}^r \cdot \vec{u}^m dS}{G_{mech}} \right)^2 \quad (10)$$

When there are perfect interfaces and all cracks are traction free, the second term in the numerator of eqn (11) vanishes leading to:<sup>5</sup>

$$G_I = G_{mech} \left( 1 + \frac{VT}{2G_{mech}} \frac{d\langle \boldsymbol{\sigma}^m \cdot \boldsymbol{\alpha} \rangle}{dA} \right)^2 \quad (11)$$

Notice here that the total  $G_I$  is a function only of the mechanical stresses ( $\boldsymbol{\sigma}^m$  and  $G_{mech}$ ). By using this equation, it is possible to completely evaluate the effect of residual thermal stresses on composite fracture without ever undertaking a thermoelastic stress analysis.<sup>5</sup> A pure mechanical stress analysis is sufficient.

## 2.2 Two Phase Isotropic

Imagine a statistically isotropic composite subjected to traction-only loading and, for simplicity, with perfect interfaces and traction-free cracks. Some examples of isotropic composites might be random, short-fiber composites, particle filled composites, or rocket propellants. The mechanical energy release rate for fracture of such a material is given by eqn (3). The residual stress effects are given by the second terms in eqn (4). The last term in eqn (4) vanishes. The result simplifies further if the isotropic composite is a two phase composite, such as a fiber/matrix composite or a particulate/matrix composites, and if each phase is isotropic. By using force balance it is possible to show that the mode I energy release rate is

$$G_I = G_{mech} \left( 1 + \frac{VT}{2G_{mech}} \Delta\alpha\Delta K \frac{d(\text{tr} \langle \boldsymbol{\varepsilon}^m \rangle)}{dA} \right)^2 \quad (12)$$

where

$$\Delta\alpha = \alpha_1 - \alpha_2 \quad \frac{1}{\Delta K} = \frac{1}{K_1} - \frac{1}{K_2} \quad \langle \boldsymbol{\varepsilon}^m \rangle = \frac{1}{V} \int_V \boldsymbol{\varepsilon}^m dV = \mathbf{S}^{(1)} v_1 \frac{d\overline{\boldsymbol{\sigma}^{(1m)}}}{dA} + \mathbf{S}^{(2)} v_2 \frac{d\overline{\boldsymbol{\sigma}^{(2m)}}}{dA} \quad (13)$$

Here  $\alpha_i$ ,  $K_i$ ,  $\mathbf{S}^{(i)}$ ,  $v_i$ , and  $\overline{\boldsymbol{\sigma}^{(im)}}$  are the thermal expansion coefficient, bulk modulus, compliance tensor, volume fraction, and phase-averaged mechanical stress in phase  $i$ . Thus the only term required to find  $G_I$  is the trace of the average mechanical strain tensor. This term is equivalent to finding the effect of damage on the effective bulk modulus of the composite.

Sometime composites crack due to residual stresses alone or they crack without the application of any mechanical stresses.<sup>6</sup> In this ‘‘thermal fracture,’’  $G_I$  can not be determined by eqn (11) because the  $G_{mech}$  in the denominator is zero. Returning to the basic definition in eqn (4), however, for a composite with perfect interfaces and traction-free cracks, the total energy release (for any mode or even mixed-mode fracture) for thermal fracture is

$$G_{res} = \frac{VT}{2} \frac{d\langle \boldsymbol{\sigma}^r \cdot \boldsymbol{\alpha} \rangle}{dA} \quad (14)$$

For a two-phase, isotropic composite with isotropic phases, this energy release rate can be written as

$$G_{res} = \frac{VT}{2} \Delta\alpha\Delta K \frac{d(\text{tr} \langle \boldsymbol{\varepsilon}^r \rangle)}{dA} \quad (15)$$

where  $\langle \boldsymbol{\varepsilon}^r \rangle$  is the average thermal strain in the composite. This term is equivalent to finding the effect of damage on the effective volumetric thermal expansion coefficient of the composite.

## 2.3 Microbond and Pull-Out Specimens

Figures 2A and 2B show the microbond test<sup>7</sup> and the single-fiber, pull-out test<sup>8</sup> that are often used to study fiber/matrix interfacial properties. In the microbond test, the fiber is pulled while a small matrix droplet is restrained with knife edges until the matrix droplet debonds from the fiber. In the single-fiber, pull-out test, the fiber is embedded in the top of a larger amount of matrix material and then pulled until the fiber/matrix interface fails. Close observations of these specimens reveal that these specimens fail by initiation and growth of interfacial cracks.<sup>9, 10</sup> In both specimens, the crack typically initiates where the fiber enters the matrix and propagates downward. Many experiments using microbond and pull-out tests are rather simplistically analyzed by calculating the average shear stress on the interface at the peak applied

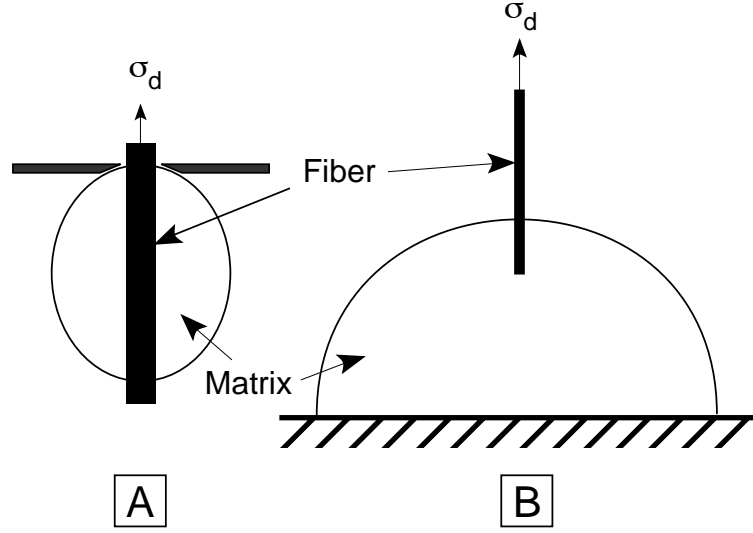


**Fig. 2.** Specimen geometries for the microbond test (A) and the single-fiber, pull out test (B).  $\sigma_d$  is the stress applied to the fiber during the test.

load and calling that result the interfacial shear strength. It is probably more realistic to analyze these tests by a fracture mechanics analysis of the propagating crack. This analysis, however, is complicated by the presence of residual stresses and by the observation of frictional loads on the debonded interface. An analysis of these specimens that uses eqn (4) and therefore accounts for both residual stresses and friction- or traction-loaded cracks is given in this section.<sup>9, 11</sup>

By applying eqn (4) to interfacial crack propagation for these two-phase model specimens, it is possible to derive an exact result for energy release rate in terms of the average axial displacements in the fiber and matrix and the phase average stresses in the fiber.<sup>9, 11</sup> After a series of approximations, all of which are expected to be very accurate for these specimens, the energy release rate for the mode II crack growth in both the microbond and the pull-out test can be written as:<sup>11</sup>

$$G(a) = \frac{r_f}{2} \left\{ C_{33s} \bar{\sigma}^2 + 2D_{3s} \bar{\sigma} T + \left( \frac{D_3^2}{C_{33}} + \frac{v_m (\alpha_T - \alpha_m)^2}{v_f A_0} \right) T^2 \right. \\ \left. - \left[ \frac{\sigma_0}{2} \left( \frac{1}{E_A} - \frac{1}{E_m} \right) + D_{3s} T \right] \left[ k C_T(a) - \left( \bar{\sigma} + \frac{(1+m)D_3 T}{C_{33}} \right) C_T'(a) \right] \right\} \quad (16)$$

Here  $a$  is the length of the interfacial crack emanating from the point where the fiber enters the matrix,  $r_f$ ,  $v_f$ ,  $\alpha_T$ , and  $E_A$  are the radius, volume fraction, transverse thermal expansion coefficient, and axial modulus of the fiber,  $v_m$ ,  $\alpha_m$  and  $E_m$  are the volume fraction, thermal expansion coefficient, and modulus of the matrix, and  $C_{33s}$ ,  $D_{3s}$ ,  $C_{33}$ ,  $D_3$ , and  $A_0$  are constants that depend only on fiber and matrix properties and on specimen geometry.<sup>11</sup> The specimen loading terms are  $\bar{\sigma}$ ,  $\sigma_0$ ,  $m$ , and  $k$ .  $\bar{\sigma}$  is a *reduced* stress defined by

$$\bar{\sigma} = \sigma_d - k a - \frac{\sigma_0 E_A}{v_f E_A + v_m E_m} \quad (17)$$

where  $\sigma_d$  is the stress applied to the fiber (see Fig. 2).  $\sigma_0$  is the *net* stress applied to the specimen which is  $\sigma_0 = 0$  for the microbond specimens and  $\sigma_0 = v_f \sigma_d$  for the pull-out test. The term  $m$  is a flag that is  $m = 0$  for the pull-out test but  $m = 1$  for the microbond test. Finally, friction on the interface is included by the term  $k$  which is defined to be

$$k = \frac{2\tau_f}{r_f} \quad (18)$$

where  $\tau_f$  is the frictional shear stress on the interfacial crack and it is assumed to be constant over the entire crack surface. The remaining unknown term is  $C_T(a)$  which is a cumulative stress-transfer function

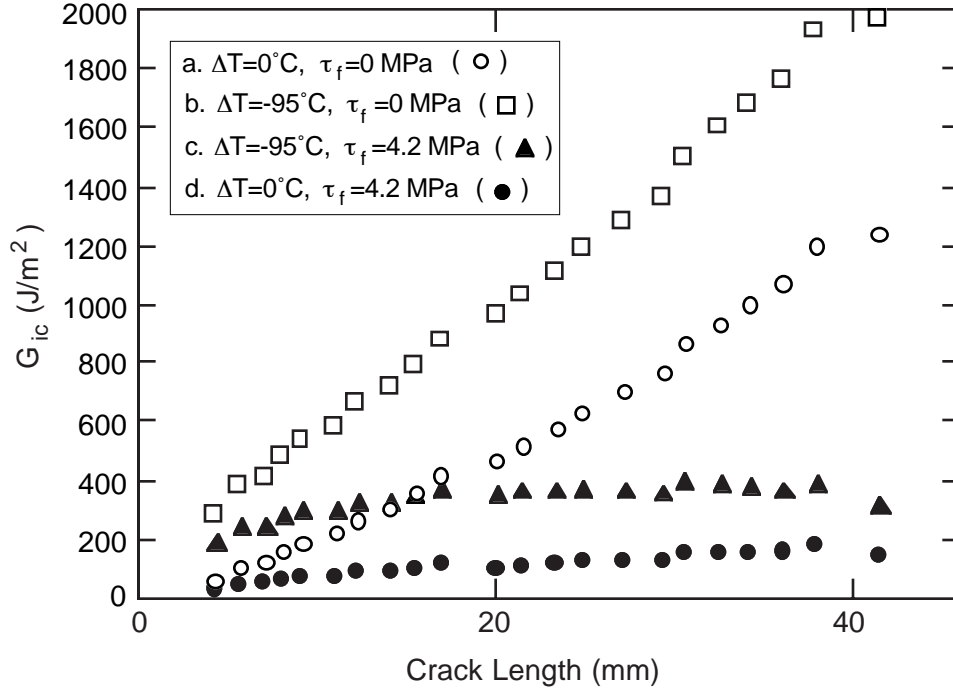


**Fig. 3.** Crack-resistance curves for a single epoxy/steel wire specimen analyzed four different ways. Curve *a* ignores residual stresses and friction; curve *b* includes residual stresses but ignores friction; curve *c* includes both residual stresses and friction; curve *d* ignores residual stresses, but includes friction.

and depends only on the average axial stress in the fiber.<sup>9, 11</sup> This function can be calculated analytically (by stress-transfer analysis), numerically (by finite element analysis), or experimentally (by Raman experiments)<sup>12</sup>. It has been shown that  $C_T(a)$  can be calculated using a simple shear-lag analysis and that the resulting  $G(a)$  agrees very well with finite element results for  $G(a)$ .<sup>9, 11</sup>

Figure (3) gives the results of using eqn (16) to interpret microbond experiments on macroscopic model specimens with steel wires embedded in cylinders of epoxy.<sup>9</sup> In these model specimens it was possible to measure debond stress,  $\sigma_d$ , as a function of crack length,  $a$ , as the interfacial crack propagated along the entire interface. For each experimental point, the results can be plugged into eqn (16) to calculate the mode II interfacial fracture toughness. This calculation can include mechanical loading only (by setting  $k = T = 0$ ), include residual stress effects only (by setting  $k = 0$  but  $T = T_s - T_0$ ), include crack-surface friction only (by setting  $k = 2\tau_f/r_f$  but  $T = 0$ ), or include both traction-loaded crack and residual stress effects (by setting  $k = 2\tau_f/r_f$  and  $T = T_s - T_0$ ). The results of all these options are given in Fig. 3. A good fracture mechanics analysis of crack growth should show that the toughness is a material property that is independent of crack length. The results in Fig. 3 show that only the unique combination of an analysis that includes both friction and residual stress effects in  $G(a)$  (see curve *c*) gives a true analysis of the experiments and thus provides an experimental result for the interfacial fracture toughness which is  $G_{II} = 360\text{ J/m}^2$ . The thermal load,  $T$ , for these specimens was calculated from the cure conditions. The friction term,  $\tau_f$ , could be measured from the residual load required to slide the epoxy cylinder along the steel wire after the entire interface had debonded.<sup>9</sup>

The analysis of microbond experiments illustrates two important points. First, residual stress effects are very important in this specimen. In fact, comparison of curves *c* and *d* show that more than half of the total energy released during crack growth is released by residual stresses. Surely any attempt to interpret microbond results that ignores residual stresses, and there have been many, will lead to a mischaracterization of the true fiber/matrix interfacial properties. Second, inclusion of frictional loads in the energy release rate is essential to the development of a fracture mechanics analysis of microbond or pull-out tests. Comparison of curves *c* and *b* show the consequence of ignoring friction. If someone used a frictionless analysis, they would conclude that fracture mechanics does not apply because  $G(a)$  is not a constant material property.

That conclusion is wrong because the friction effect depends on crack length. As the crack length gets longer the total frictional load increases. This increased load causes an *apparent*  $G(a)$  to increase as the crack length gets longer. The *true* toughness, however, must be calculated by subtracting the frictional effects to get the actual amount of energy released as the crack grows.

These above arguments are relevant to friction effects and imperfect interface effects in all types of composite fracture. There is a tendency in analysis of composite fracture to consider friction effects or sliding at imperfect interfaces as *toughening* mechanisms that can lead to composite materials with enhanced toughness properties. Such an *increase* in toughness, however, is only an increase in an *effective* or *apparent* toughness. It is observed by conducting experiments on materials in which friction or imperfect interface effects are important but then calculating toughness by an energy release rate analysis that ignores those effects. In other words, the calculated toughness uses an invalid analysis that does not correspond to the *true* amount of energy released during crack growth. One could argue that friction and imperfect interfaces are internal effects that should be included in the toughness of the material instead of in the energy release rate for crack growth. In other words, they are effects that can be exploited to develop tougher materials. The danger of this approach is that friction and imperfect interface effects are not local to the crack tip and thus not independent of the current state of damage. As a consequence, the material toughness will no longer be a material property but will depend on specimen geometry and on current damage state. In other words, interpreting friction and imperfect interface effects as toughening mechanisms defeats the purpose of using fracture mechanics to study composite fracture. Despite these comments, friction and imperfect interface effects can lead to materials with enhanced load-carrying capabilities in the presence of damage. They provide improvements, however, by reducing energy release rate for crack growth and not by increasing the amount of energy dissipated during crack growth. The difference might appear to be one of semantics, but it is actually essential to the development of sound fracture mechanics analyses of composite fracture.

## 2.4 Finite Fracture Mechanics

Another complication of composite fracture mechanics analysis is that many failure processes are characterized by fracture events instead of by continuous crack growth. Typical fracture events are fiber breaks, matrix cracks,<sup>13, 14</sup> and instantaneous fiber/matrix debonding.<sup>15</sup> Conventional fracture mechanics deals with predicting the conditions for which an existing crack will propagate into a larger crack. The experimental reality for composites is that crack growth is often not observable; all that can be observed is the occurrence of fracture events. When no experimental observations for crack growth are possible, there are two alternatives. Either one can abandon fracture mechanics or one has to develop new fracture mechanics methods for predicting fracture events. Failure models that ignore fracture mechanics are typically not very successful. This section considers the alternative of developing new fracture mechanics methods. Because fracture events are associated with a finite increase in fracture area, Hashin has suggested calling such an analysis finite fracture mechanics.<sup>16</sup> This section paper outlines some mathematical methods for finite fracture mechanics, points out a new observation about boundary condition effects, and gives an example by analyzing matrix microcracking.<sup>4, 17</sup>

In finite fracture mechanics, one assumes that traditional fracture mechanics methods still apply. In other words, it is assumed that the next fracture event will occur when the total energy released per unit new fracture area,  $\Delta A$ , exceeds some toughness or critical energy release rate for that event. One difference, is that energy release rate in eqn (1) must now be calculated from a discrete derivative

$$\Delta G = -\frac{\Delta \Pi}{\Delta A} = \frac{\Delta(W - U - K)}{\Delta A} \quad (19)$$

The finite energy release rate,  $\Delta G$ , is the change in potential energy,  $\Delta \Pi$ , per unit area,  $\Delta A$ . A second change is that even in static loading, each fracture event may be associated with some kinetic energy,  $\Delta K$ . Kinetic energy effects are apparent by the observation of acoustic emissions associated with events. The new kinetic energy term presents a problem because it will typically be impossible to calculate. There are two key situations, however, where it can be ignored and thus where there are opportunities for finite fracture mechanics models of composite failure. First,  $\Delta K$  may be small, or, second,  $\Delta K$  may be a characteristic of the event being analyzed. In either case, we can calculate finite energy release rate from the simpler formula  $\Delta G = \Delta(W - U)/\Delta A$  and assume the next fracture event will occur when  $\Delta G \geq \Delta G_c$  where  $\Delta G_c$  is the

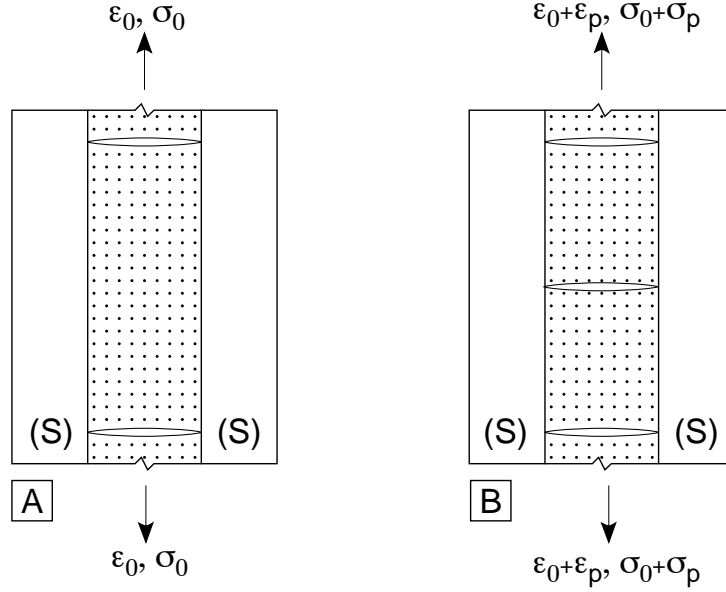


**Fig. 4.** A unit cell of damage for microcracking in  $[(S)/90_n]_s$  laminates where  $(S)$  is any supporting sub-laminate. A. Two existing microcracks. B. The same laminate after formation of a new microcrack between the existing microcracks.

critical energy release rate for that particular fracture event. If  $\Delta K$  is small, then  $\Delta G_c$  will be the average toughness for the crack growth that formed the entire event. If  $\Delta K$  is not small but nearly constant for all such events, then finite fracture mechanics is including  $\Delta K/\Delta A$  as part of the event toughness. Thus,  $\Delta G_c$  becomes an *effective* material property that includes but actual toughness and kinetic energy effects.

#### 2.4.1 Matrix Microcracking

When cross-ply laminates ( $[0_n/90_m]_s$  or  $[90_m/0_n]_s$ ) are loaded in tension parallel to the  $0^\circ$  plies, the  $90^\circ$  plies develop transverse cracks or matrix microcracks (see review articles Refs. 13 and 14). On continued loading, the  $90^\circ$  plies crack into a roughly periodic array of microcracks. Early work on microcracking suggested microcracks form when the stress in the  $90^\circ$  plies reaches the transverse strength of the plies.<sup>18</sup> Strength models, however, do a poor job of explaining experimental results.<sup>14, 19</sup> It is now accepted that microcracking experiments can be better explained by a finite fracture mechanics model that assumes the next microcrack forms when the finite energy release rate,  $\Delta G_m$ , for formation of that microcrack reaches  $G_{mc}$  or the critical microcracking toughness of the composite.<sup>13, 14, 19</sup>

The key problem to analyze is to calculate the change in energy on going from the initial state in Fig. 4A to the new state in Fig. 4B following the formation of a new microcrack. This energy release rate can be calculated by a discrete form of eqn (7) or

$$\Delta G_m = \frac{1}{\Delta A} \left( \int_{S_c} \vec{T}^p \cdot \vec{u}^0 dS + \frac{1}{2} \int_V \sigma^p \mathbf{S} \sigma^p dV \right) \quad (20)$$

Here the initial stress are the stresses in Fig. 4A while the perturbation stress are the change in stresses on forming the new microcrack in Fig. 4B. The problem of finding  $\Delta G_m$  has been discussed in many papers<sup>13, 14</sup> and will not be discussed here. We state only that  $\Delta G_m$  can be bounded using variational mechanics methods<sup>4</sup> and that an average of those bounds provides an essentially exact result.<sup>20</sup>

However  $\Delta G_m$  is found, it is convenient to express it in a normalized form of

$$\Delta G_m = (\sigma_{xx,1}^0)^2 G_{m,unit}(D) \quad (21)$$

where  $\sigma_{xx,1}^0$  is the stress in the  $90^\circ$  plies in the absence of any microcracks and  $G_{m,unit}(D)$  is the energy release rate when there is unit initial axial stress in the  $90^\circ$  plies ( $\sigma_{xx,1}^0 = 1$ ) and the current crack density

is  $D$ . In linear thermoelasticity,  $\sigma_{xx,1}^0$  can be written as  $\sigma_{xx,1}^0 = k_m^{(1)}\sigma_0 + k_{th}^{(1)}T$  where  $\sigma_0$  is total applied stress and  $k_m^{(1)}$  and  $k_{th}^{(1)}$  are mechanical and thermal stiffness terms that can be derived from laminated plate theory.<sup>13</sup> Equating  $\Delta G_m$  to  $G_{mc}$  and rearranging gives

$$-\frac{k_m^{(1)}}{k_{th}^{(1)}}\sigma_0 = -\frac{1}{k_{th}^{(1)}}\sqrt{\frac{G_{mc}}{G_{m,unit}(D)}} + T \quad (22)$$

This equation suggests defining reduced stress and reduced crack density<sup>19</sup> as

$$\sigma_{red} = -\frac{k_m^{(1)}}{k_{th}^{(1)}}\sigma_0 \quad \text{and} \quad D_{red} = -\frac{1}{k_{th}^{(1)}}\sqrt{\frac{1}{G_{m,unit}(D)}} \quad (23)$$

which leads to

$$\sigma_{red} = D_{red}\sqrt{G_{mc}} + T \quad (24)$$

For a given laminate material, eqn (24) defines a microcracking master plot.<sup>19</sup> When a collection of experimental results from a variety of laminates of the same material are plotted as a master plot, eqn (24) predicts the resulting plot should be linear with a slope of  $\sqrt{G_{mc}}$  and an intercept giving the residual stress term  $T$ .<sup>19</sup> A master plot analysis of microcracking experiments critically tests the fundamental finite fracture mechanics hypothesis that the toughness property,  $G_{mc}$ , can be treated as a material property, or at least an *effective* material property, that is independent of the laminate structure and the current damage state. Moreover, a master plot analysis can be done with any input theory for  $G_{m,unit}(D)$  and thus can also test the validity of the stress analysis used to find  $\Delta G_m$ .<sup>14</sup>

Figure 5 gives a master plot for 14 different laminates of AS4/3501-6 carbon/epoxy laminates. This master plot analysis was constructed using a  $G_{m,unit}(D)$  calculated using complementary energy methods and variational mechanics.<sup>13, 14, 21</sup> Previous master plot calculations assumed constant load boundary conditions, but these experiments were under displacement control.<sup>19</sup> Therefore,  $G_{m,unit}(D)$  was adjusted to account for displacement-control experiments.<sup>4, 14, 17</sup> This master plot is linear within a narrow experimental scatter band. The results for all laminates fall on the same line. Notably, the raw experimental results for  $[0_n/90_m]_s$  and  $[90_m/0_n]_s$  laminates with the same values of  $m$  and  $n$  are different, but the analyses converge to the same master plot. In other words, finite fracture mechanics analysis of microcracking can explain the difference in microcracking properties for laminates with central 90° plies *vs.* laminates with surface 90° plies. From the slope and intercept of the master plot, the microcracking toughness is found to be  $G_{mc} = 220 \text{ J/m}^2$  and the residual stress term is found to be  $T = -95^\circ\text{C}$ .<sup>14</sup> Both of these results are physically reasonable which further supports the validity of the finite fracture mechanics model of microcracking. Note that master plot analysis lets one determine toughness without any prior knowledge of the level of residual stresses in the laminate. The level of residual stresses are experimentally determined during analysis of the microcracking experiments from the intercept of the master plot.

Figure 5 shows that finite fracture mechanics models of composite fracture events can provide an excellent tool for analysis of composite damage. There are two key points that are discovered in more detailed analyses of the microcracking problem.<sup>13, 14, 19</sup> First, analysis of composite microcracking requires stress analysis methods that give accurate results for  $\Delta G_m$ . Some early models of composite microcracking relied on shear-lag methods. Although shear-lag methods do an excellent job of calculating the effect of microcracks on effective axial modulus,<sup>22</sup> they are much less accurate for calculation of energy release rate.<sup>13, 14, 19</sup> As illustrated in Fig. 1, calculation of energy release rate requires calculation of *derivatives* of effective properties. Because of the nature of differentiation, any errors in finding effective properties may get greatly magnified when finding their derivatives. As a consequence, verification of a damage mechanics model showing that it can predict the effect damage on effective modulus is insufficient justification for use of that model in fracture mechanics calculations. Before any model can be used in fracture mechanics models, it must be verified that it can accurately handle the more-difficult problem of finding derivatives with respect to damage area.

Beside the extra accuracy requirements for fracture mechanics models, those models need to account for boundary condition effects. In traditional fracture mechanics with infinitesimal amounts of crack growth, the energy release rate is independent of whether the experiments are conducted under load-control or displacement-control conditions. The situation changes for finite fracture mechanics.<sup>4, 14, 17</sup> The finite fracture problem is illustrated schematically in Fig. 6. In finite fracture the hysteresis area between the loading

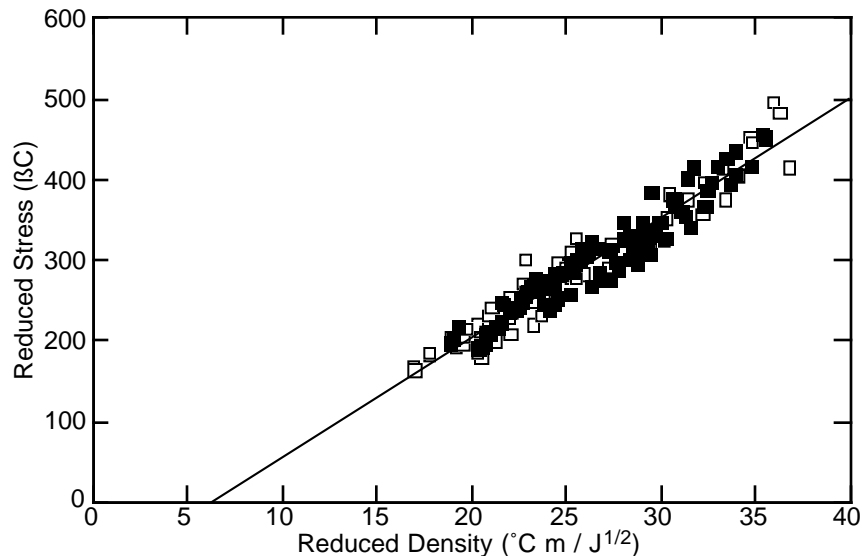


**Fig. 5.** Master plot analysis for 14  $[0_n/90_m]_s$  (open symbols) and  $[90_m/0_n]_s$  (filled symbols) AS4/3501-6 carbon/epoxy laminates.  $G_{m,unit}(D)$  was calculated from a complementary energy analysis with constant-displacement boundary conditions. The straight line is a linear fit to the experimental results. The slope and intercept of the fit give  $G_{mc} = 220 \text{ J/m}^2$  and  $T = -95^\circ\text{C}$ .

and unloading curves must be equal to the total energy released by the finite increase in fracture area between the loading experiment and the unloading experiment. When the experiment is done under load-control conditions, the total energy released will be given by the area of the  $ABC$  triangle (see Fig. 6). If the same amount of fracture area is generated in a displacement-control experiment, however, the total energy released will be given by the area of the  $ABD$  triangle. In brief, finite energy release rate is affected by loading conditions — displacement-control experiments release less energy than load-control experiments for conditions when the formation of damage occurs at the same initial load. Both experiments and analysis for the results in Fig. 5 used displacement-control conditions. Previous analyses of microcracking used load-control stress analysis on experiments that were done under displacement control.<sup>13, 19</sup> Because the boundary condition effects are not large in microcracking, these flawed models still worked reasonably well.<sup>19</sup> The preferred analyses of microcracking, and the analyses that give the *true* result for  $G_{mc}$ , should match the theoretical model boundary conditions with the experimental boundary conditions.<sup>4, 14</sup>

The second point is that finite fracture mechanics analysis of microcracking is the only method that can correlate experimental results for a wide range of laminates on a single master plot. In other words, by using fracture mechanics, a single result for  $G_{mc}$  can be used to predict microcracking experiments in a wide variety of lay ups. An alternate approach to predicting microcracking events is to assume the next microcrack forms when the stress in the  $90^\circ$  plies becomes equal to the strength of these plies. It is possible to cast strength models in a master-plot form analogous to the master plot used for the finite fracture mechanics model.<sup>19</sup> When a strength master plot is used to interpret experiments, however, the results are very poor.<sup>19, 14</sup> The results for individual laminates provide reasonable results with the slope now providing an *effective* strength of the  $90^\circ$  plies and the intercept providing the magnitude of the residual stresses. When several laminates are analyzed together, however, the results do not converge to a single master plot. In other words, there is no such thing as a *ply strength* that determines the onset of microcracking. Strength models must resort to treating ply strength as an *in situ* property that is different for every lay up. The use of *in situ* properties severely limits the utility of strength models. In contrast, a finite fracture mechanics model does not need *in situ* properties and thus provides a much more compelling and fundamental understanding of the microcracking process.

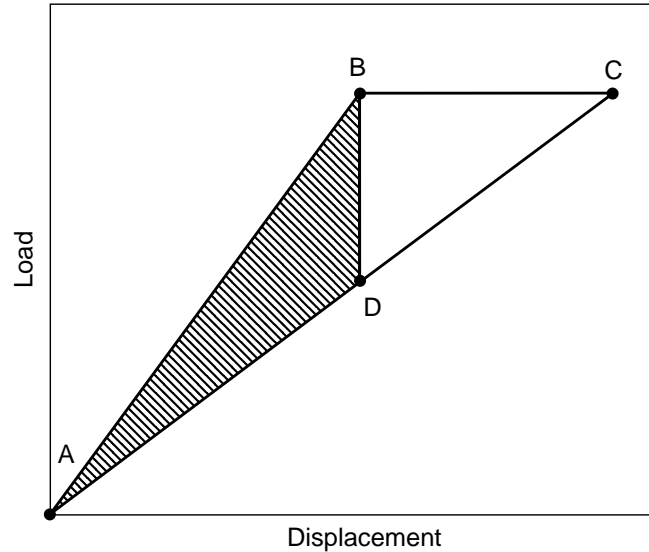


**Fig. 6.** Load-displacement curve for a finite increase in crack area. The area of the  $ABC$  triangle is the total energy released by crack growth under load control. The shaded area of the  $ABD$  triangle is the total energy released by crack growth under displacement control.

### 3 CONCLUSIONS

Many composites, especially those with continuous, aligned, high-modulus fibers, are close to being linear elastic until failure. Such composites are thus excellent candidates for failure analysis using linear elastic fracture mechanics, in which failure is assumed to occur when the energy release rate,  $G$ , for damage growth exceeds the critical energy release rate,  $G_c$ , or toughness of the material. In other words, failure analysis of composites can often be reduced to the problem of calculating  $G$  for some particular type of damage growth. The calculation of  $G$  for composites, however, is normally more complicated than for homogeneous materials because it must account for material heterogeneity, residual stresses caused by differential phase shrinkage, tractions, such as friction, on some crack surfaces, and for possibly imperfect interfaces. This paper has outlined some new methods for fracture mechanics calculations in composites that account for all possible composite effects in energy release rate. These new methods were applied to several composite fracture problems and to the analysis of fracture events using a new concept called “finite fracture mechanics.” A key point in composite fracture analysis is that friction and imperfect interface effects should be part of the energy release rate and not part of the material toughness. Two key points in finite fracture mechanics are that the stress analysis methods must be accurate for *derivatives* of effective properties (not just the effective properties themselves) and must correctly match the boundary conditions used during the experiments.

### ACKNOWLEDGEMENTS

This work was supported, in part, by a grant from the Mechanics of Materials program at the National Science Foundation (CMS-9713356), and, in part, by the University of Utah Center for the Simulation of Accidental Fires and Explosions (C-SAFE), funded by the Department of Energy, Lawrence Livermore National Laboratory, under Subcontract B341493.

### REFERENCES

1. J. G. Williams, *Fracture Mechanics of Solids*, John Wiley & Sons, New York, 1984.
2. J. A. Nairn and P. Zoller, Matrix Solidification and the Resulting Residual Thermal Stresses in Composites. *Journal of Material Science*, **20** (1985) 355–367.

3. Z. Hashin, Thermoelastic Properties of Fiber Composites With Imperfect Interface. *Mechanics of Materials*, **8** (1990) 333–348.
4. J. A. Nairn, Exact and Variational Theorems for Fracture Mechanics of Composites with Residual Stresses, Traction-Loaded Cracks, and Imperfect Interfaces. *Int. J. Fract.*, (1999) in press.
5. J. A. Nairn, Fracture Mechanics of Composites With Residual Thermal Stresses. *Journal of Applied Mechanics*, **64** (1997) 804–810.
6. H. W. Kim, M. A. Grayson, and J. A. Nairn, The Effect of Hygrothermal Aging on the Microcracking Properties of Some Carbon Fiber/Polyimide Laminates. *Adv. Comp. Letters*, **4** (1995) 185–188.
7. B. Miller, Muri, P., and Rebenfeld, L., A Microbond Method for Determination of the Shear Strength of a Fiber/Resin Interface. *Comp. Sci. & Tech.*, **28** (1987) 17–32.
8. L. S. Penn, and Bowler, E. R., A New Approach to Surface Energy Characterization for Adhesive Performance Prediction. *Surf. Interf. Anal.*, **3** (1981) 161–164.
9. C. H. Liu and J. A. Nairn, Analytical Fracture Mechanics of the Microbond Test Including the Effects of Friction and Thermal Stresses. *J. of Adhes. and Adhesives*, **19** (1999) 59–70.
10. S. Mertz, Auersch, W., Marotzke, C., Schulz, E., and Hampe, A., Investigation of Morphology-Dependent Fracture Behaviour with the Single-Fibre Pull-Out Test. *Comp. Sci. & Tech.*, **48** (1993) 285–290.
11. J. A. Nairn, Analytical Fracture Mechanics Analysis of the Pull-Out Test Including the Effects of Friction and Thermal Stresses. *Adv. Comp. Letts.*, (2000) in press.
12. M. C. Andrews, Bannister, D. J., and Young, R. J., Review: The Interfacial Properties of Aramid/Epoxy Model Composites. *J. Mat. Sci.*, **31** (1996) 3893–3913.
13. J. A. Nairn and S. Hu, Micromechanics of Damage: A Case Study of Matrix Microcracking. In: *Damage Mechanics of Composite Materials* (edited by R. Talreja ), Elsevier, Amsterdam, 1994, 187–243.
14. J. A. Nairn, Matrix Microcracking in Composites. In: *Polymer Matrix Composites, vol. 2 of Comprehensive Composite Materials* eds., edited by R. Talreja and J.-A. E. Manson, Elsevier Science, 2000, 403–432.
15. X.-F. Zhou, J. A. Nairn, and H. D. Wagner, Fiber-Matrix Adhesion From the Single-Fiber Composite Test: Nucleation of Interfacial Debonding. *Composites*, **30** (1999) 1387–1400.
16. Z. Hashin, Finite Thermoelastic Fracture Criterion with Application to Laminate Cracking Analysis. *Journal of the Mechanics and Physics of Solids*, **44** (1996) 1129–1145.
17. J. A. Nairn, Applications of Finite Fracture Mechanics for Predicting Fracture Events in Composites. *Fifth Int'l Conf. on Deformation and Fracture of Composites*, London, UK, March 18-19, 1999, 1–10.
18. K. W. Garrett and J. E. Bailey, Multiple Transverse Fracture in 90 Cross-Ply Laminates of a Glass Fibre-Reinforced Polyester. *J. Mat. Sci.*, **12** (1977) 157–168.
19. J. A. Nairn, S. Hu, and J. S. Bark, A Critical Evaluation of Theories for Predicting Microcracking in Composite Laminates. *Journal of Material Science*, **28** (1993) 5099–5111.
20. J. A. Nairn, Some New Variational Mechanics Results on Composite Microcracking. *Proceedings of the 10<sup>th</sup> International Conference on Composite Materials*, **I** (1995) 423–430.
21. Z. Hashin, Analysis of Cracked Laminates: A Variational Approach. *Mechanics of Materials*, **4** (1985) 121–136.
22. L. N. McCartney, Analytical Models of Stress Transfer in Unidirectional Composites and Cross-Ply Laminates, and Their Application to the Prediction of Matrix/Transverse Cracking. In: *Local Mechanics Concepts for Composite Material Systems* eds., J. N. Reddy and K. L. Reifsnider, Proc. IUTAM Symposium, Blacksburg, VA, 1991, 251–282.